Electronic Supplementary Information (ESI) available for:

Impact of hole doping on spin transition in perovskite-type cobalt oxides

Xiangli Che, Liping Li, Wanbiao Hu, and Guangshe Li*

Key Laboratory of Design and Assembly of Functional Nanostructures, Fujian Institute of Research on the Structure of Matter, Chinese Academy of Sciences. Fuzhou, 350002, P.R.China.

Table S1. Chemical composition of the PrCo1-xNixO3-δ (*x*=0~0.4) phases.

x	Cationic composition (ICP)		Oxygen content	
	Co	Ni	Iodometric titration	TPR
0	1	-	3.00±0.001	3.002±0.003
0.1	0.90±0.03	0.10±0.01	2.94±0.02	2.950±0.001
0.2	0.80±0.02	0.20±0.01	2.89±0.02	2.898±0.002
0.3	0.70±0.02	0.30±0.01	2.85±0.02	2.849±0.002
0.4	0.60±0.02	0.40±0.01	2.80±0.04	2.796±0.005

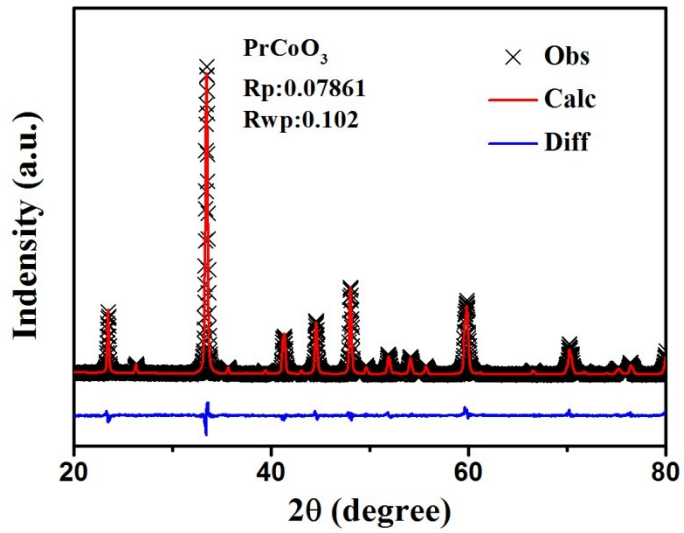

Fig. S1 Typical Rietveld structural refinements of powder X-ray diffraction data for the x=0 sample

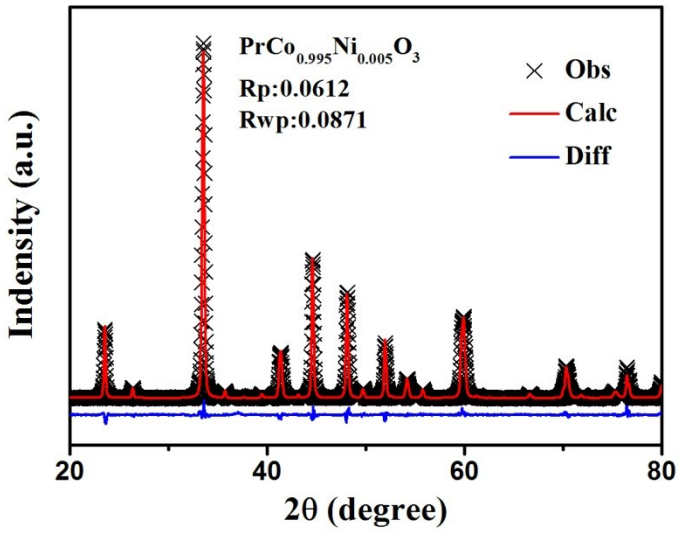

Fig. S2 Typical Rietveld structural refinements of powder X-ray diffraction data for the x=0.005 sample

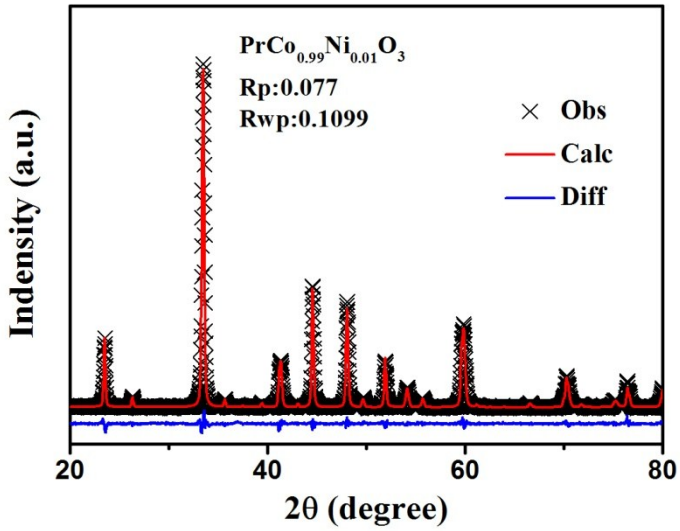

Fig. S3 Typical Rietveld structural refinements of powder X-ray diffraction data for the x=0.01 sample

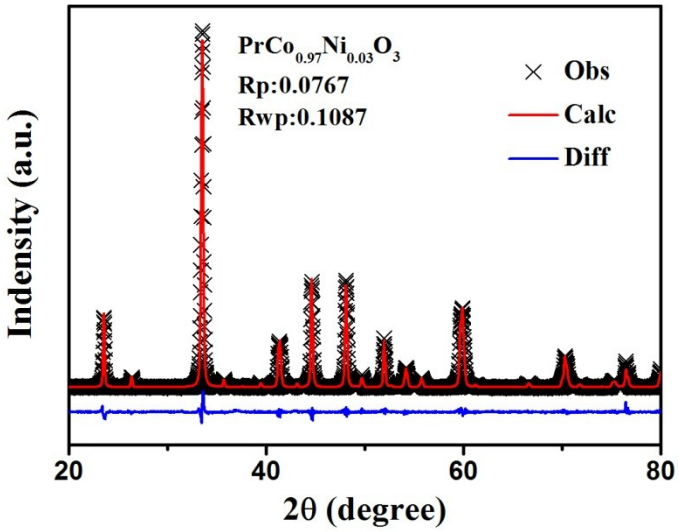

Fig. S4 Typical Rietveld structural refinements of powder X-ray diffraction data for the x=0.03 sample

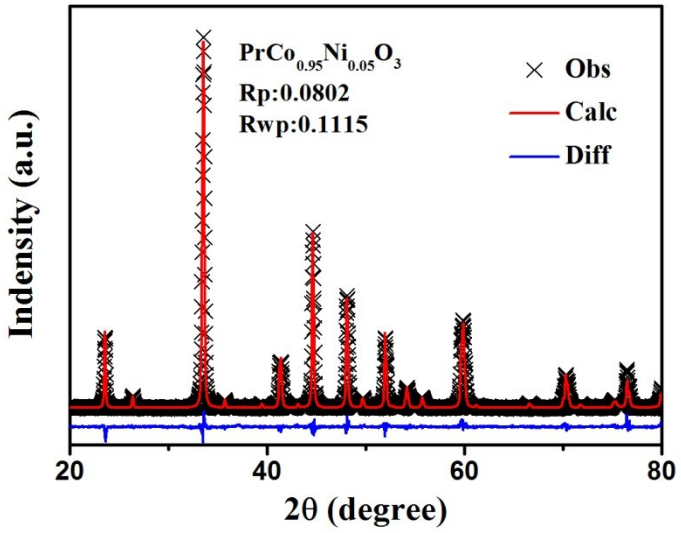

Fig. S5 Typical Rietveld structural refinements of powder X-ray diffraction data for the x=0.05 sample

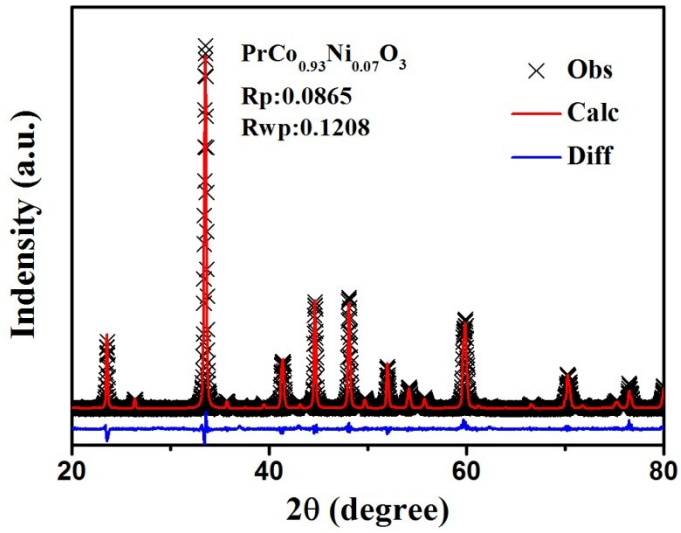

Fig. S6 Typical Rietveld structural refinements of powder X-ray diffraction data for the x=0.07 sample

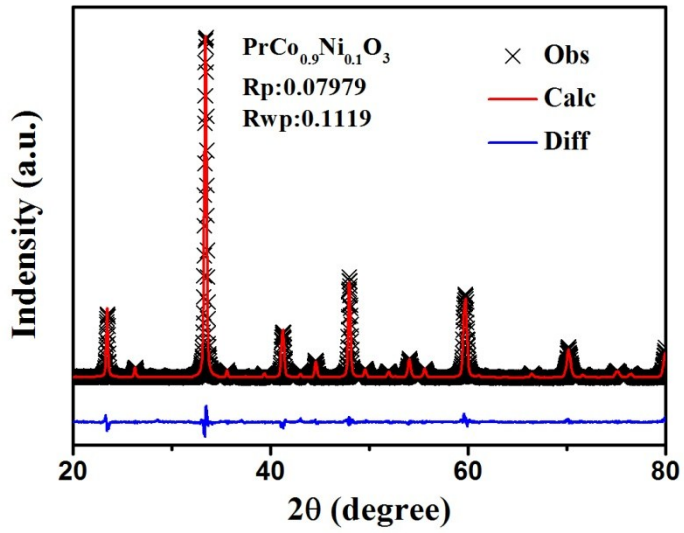

Fig. S7 Typical Rietveld structural refinements of powder X-ray diffraction data for the x=0.1 sample

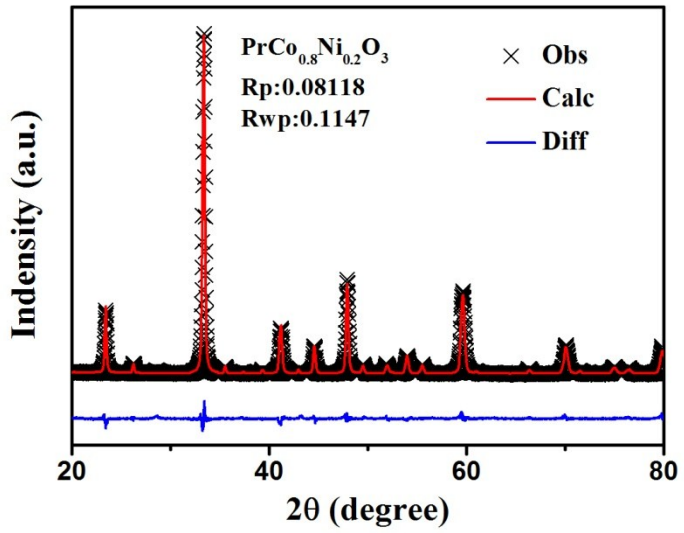

Fig. S8 Typical Rietveld structural refinements of powder X-ray diffraction data for the x=0.2 sample

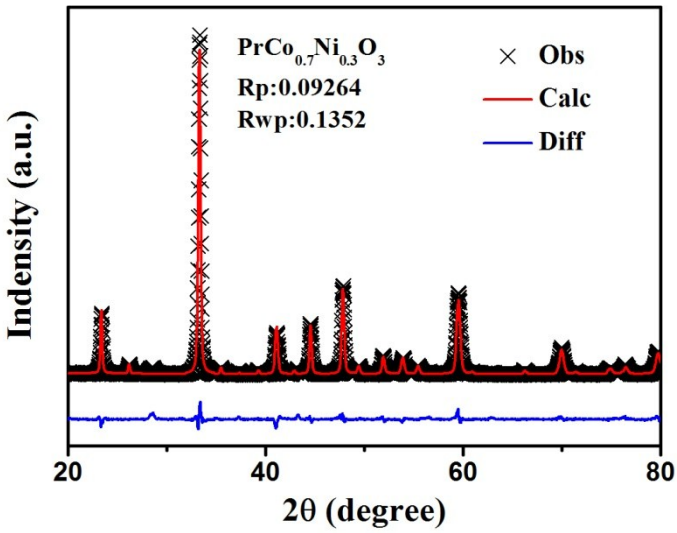

Fig. S9 Typical Rietveld structural refinements of powder X-ray diffraction data for the x=0.3 sample

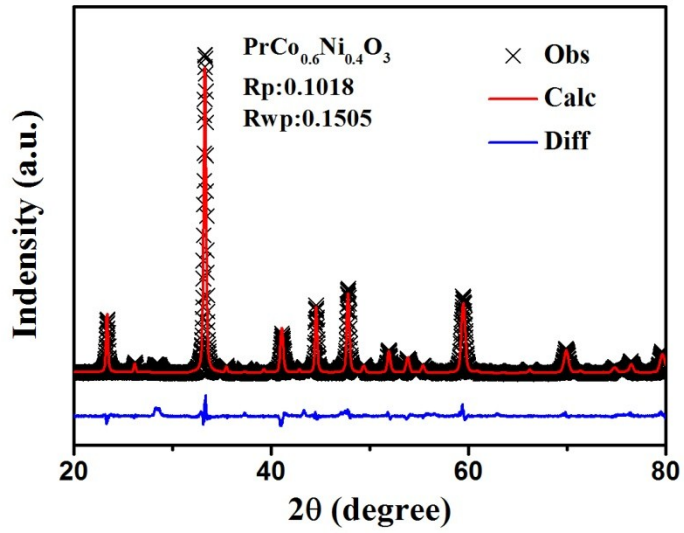

Fig. S10 Typical Rietveld structural refinements of powder X-ray diffraction data for the x=0.4 sample

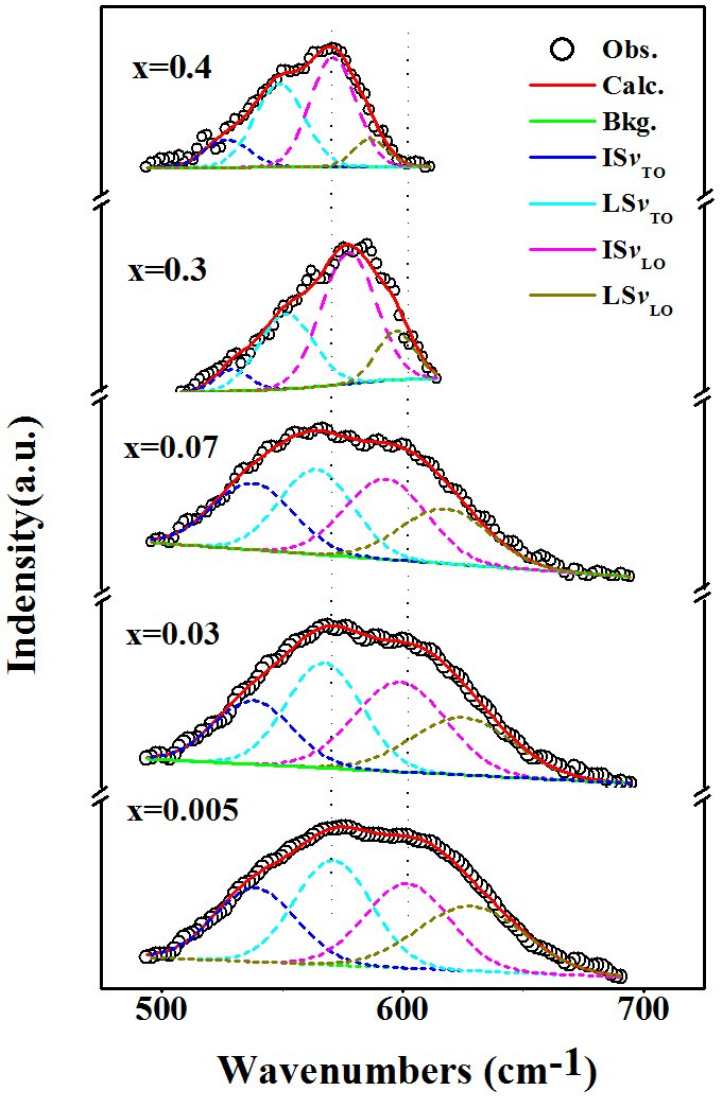

Fig. S11 IR spectra of the $PrCo_{1-x}Ni_xO_{3-\delta}$（$x$=0~0.4）samples at given x

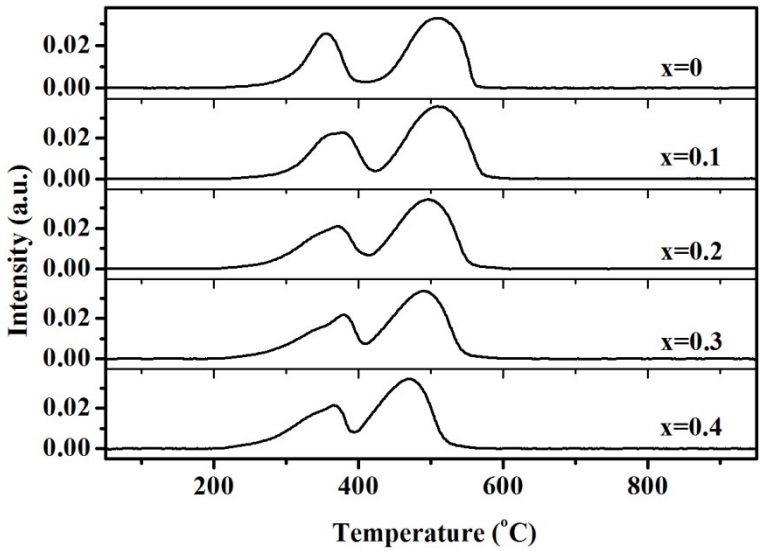

Fig. S12 TPR profiles for the $PrCo_{1-x}Ni_xO_{3-\delta}$（*x*=0~0.4）samples at given *x*

Fig. S12 shows the TPR profiles of $PrCo_{1-x}Ni_xO_{3-\delta}$（*x*=0~0.4）samples. We can see that all samples have two reduction peaks, which correspond to two-step reduction process. The 11.9 mg of CuO was chosen as the standard sample to evaluate the hydrogen consumption of $PrCo_{1-x}Ni_xO_{3-\delta}$（*x*=0~0.4）and Pr_6O_{11} samples. Furthermore, through calculating the hydrogen consumption of Pr_6O_{11}, we can judge the Pr_6O_{11} was completely reduced to Pr_2O_3 after TPR, so the Pr^{3+} is stable in this test process. This result is similar to that reported in previous literatures.[1, 2] So we can obtain following reduction reaction processes.

$$2\ Pr^{3+}_{1-x}M^{2+}_{x}\ O_{3-\delta} + (1-x)/2\ H_2 \rightarrow 2\ PrM^{2+}O_{2.5-\delta+x/2} + (1-x)/2\ H_2O \quad (1)$$

$$2\ PrM^{2+}O_{2.5-\delta+x/2} + 2H_2 \rightarrow Pr_2O_3 + M + 2H_2O \quad (2)$$

Base on the total consumption of H_2 corresponds to the first step and the second step, we can obtain the oxygen content of $PrCo_{1-x}Ni_xO_{3-\delta}$, furthermore, the valences of the transition metal ions oxygen can be calculated combining the results of ICP.

Reference:

1. M. Futai and C. Yonghua, *React. Kinet. Catal. Lett.*, 1986, **31**, 47-54.

2. S. Royer, H. Alamdari, D. Duprez and S. Kaliaguine, *Appl. Catal., B*, 2005, **58**, 273-288.